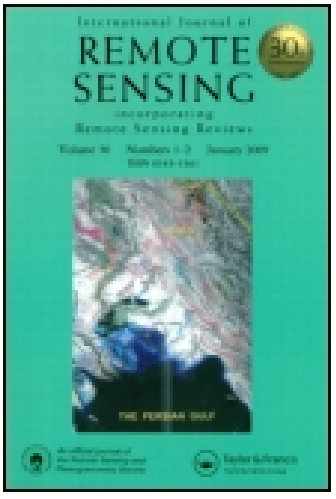

International Journal of Remote Sensing
Publication details, including instructions for authors and subscription information:
http://www.tandfonline.com/loi/tres20

Monitoring surface water content using visible and short-wave infrared SPOT-5 data of wheat plots in irrigated semi-arid regions

Tarik Benabdelouahab[ab], Riad Balaghi[a], Rachid Hadria[a], Hayat Lionboui[a], Julien Minet[b] & Bernard Tychon[b]

[a] Département de l'Environnement et Ressources Naturelles, National Institute of Agronomic Research, Rabat, Morocco

[b] Unité de recherche Eau - Environnement - Développement, Université de Liège (ULg), Arlon Campus, Arlon, Belgium

Published online: 30 Jul 2015.

To cite this article: Tarik Benabdelouahab, Riad Balaghi, Rachid Hadria, Hayat Lionboui, Julien Minet & Bernard Tychon (2015) Monitoring surface water content using visible and short-wave infrared SPOT-5 data of wheat plots in irrigated semi-arid regions, International Journal of Remote Sensing, 36:15, 4018-4036, DOI: 10.1080/01431161.2015.1072650

To link to this article: http://dx.doi.org/10.1080/01431161.2015.1072650

International Journal of Remote Sensing, 2015
Vol. 36, No. 15, 4018–4036, http://dx.doi.org/10.1080/01431161.2015.1072650

Monitoring surface water content using visible and short-wave infrared SPOT-5 data of wheat plots in irrigated semi-arid regions

Tarik Benabdelouahab[a,b]*, Riad Balaghi[a], Rachid Hadria[a], Hayat Lionboui[a], Julien Minet[b], and Bernard Tychon[b]

[a]*Département de l'Environnement et Ressources Naturelles, National Institute of Agronomic Research, Rabat, Morocco;* [b]*Unité de recherche Eau - Environnement - Développement, Université de Liège (ULg), Arlon Campus, Arlon, Belgium*

(*Received 28 October 2014; accepted 10 July 2015*)

Irrigated agriculture is an important strategic sector in arid and semi-arid regions. Given the large spatial coverage of irrigated areas, operational tools based on satellite remote sensing can contribute to their optimal management. The aim of this study was to evaluate the potential of two spectral indices, calculated from SPOT-5 high-resolution visible (HRV) data, to retrieve the surface water content values (from bare soil to completely covered soil) over wheat fields and detect irrigation supplies in an irrigated area. These indices are the normalized difference water index (NDWI) and the moisture stress index (MSI), covering the main growth stages of wheat. These indices were compared to corresponding *in situ* measurements of soil moisture and vegetation water content in 30 wheat fields in an irrigated area of Morocco, during the 2012–2013 and 2013–2014 cropping seasons. NDWI and MSI were highly correlated with *in situ* measurements at both the beginning of the growing season (sowing) and at full vegetation cover (grain filling). From sowing to grain filling, the best correlation (R^2 = 0.86; $p < 0.01$) was found for the relationship between NDWI values and observed soil moisture values. These results were validated using a *k*-fold cross-validation methodology; they indicated that NDWI can be used to estimate and map surface water content changes at the main crop growth stages (from sowing to grain filling). NDWI is an operative index for monitoring irrigation, such as detecting irrigation supplies and mitigating wheat water stress at field and regional levels in semi-arid areas.

1. Introduction

Half of the world's food supply comes from irrigated areas that use about 72% of the available water resources (Geerts and Raes 2009; Seckler, Barker, and Amarasinghe 1999). In Morocco, water availability is the main limiting factor for crop production, and it is becoming a national priority for the agricultural sector (Lionboui et al. 2014). This situation has led to work on developing optimum strategies for planning and managing available water resources. Cereal (wheat and barley) production is strongly linked to the amount and distribution of rainfall in rainfed areas (Balaghi et al. 2013), and to the amount of groundwater and water stored in dams for irrigated areas. A set of irrigated areas in the country was equipped with the means to improve and secure crop production. Despite the large amounts of irrigation water consumed, wheat yields in irrigated areas remain low and fluctuate from one season to another due to fluctuating water availability and non-optimal management practices (Balaghi et al. 2010). In the

*Corresponding author. Email: Tarik.benabdelouahab@gmail.com

current context of climate change, water scarcity, and population growth, managing irrigation water has become a critical issue.

In Morocco, the Tadla irrigated area is managed by the Regional Office for Agricultural Development of Tadla (ORMVAT). The main cultivated crop in this area is wheat, covering more than 40,000 hectares (ha), which represent more than 36% of the total irrigated area (ORMVAT 2009). ORMVAT is seeking a spatio-temporal methodology for monitoring surface water content for improving irrigation scheduling and preventing agricultural water stress (Er-Raki, Chehbouni, and Duchemin 2010; Ozdogan et al. 2010). In addition, this could also be profitable for detecting uncontrolled irrigation and illegal water pumping.

Remotely sensed reflectance has been used to estimate soil and vegetation water content for various crops and to monitor water irrigation per surface unit (Ben-Gal et al. 2010; Ceccato, Flasse, and Grégoire 2002; Cheng et al. 2012; Hadria et al. 2010; Penuelas et al. 1997; Tian et al. 2001; Trombetti et al. 2008), drawing on the high temporal and spatial resolution of satellite images. Several indices based on wavelengths ranging between 400 and 2500 nm have been developed to describe land-surface moisture conditions (Kogan 2000). Estimation of surface water content values from remote-sensing data is usually based on reflectance in the red (R; 610–680 nm), near infrared (NIR; 780–890 nm), and short-wave infrared (SWIR; 1580–1750 nm) regions of the spectrum (Lobell et al. 2003; Muller and Décamps 2001; Skidmore, Dickerson, and Shimmelpfennig 1975; Moreno et al. 2014).

During the wheat development cycle, crop water stress can be deduced from both vegetation and soil water content (Feng et al. 2013; Ghulam et al. 2007; Ning et al. 2013). Water stress indices used for crop management should therefore be based on the spectral bands that are sensitive to both soil moisture and vegetation water content.

Many indices for the simultaneous estimation of vegetation water content and soil moisture have been proposed for different land surfaces, from bare soils to vegetated areas, among which are the visible and short-wave infrared drought index (VSDI; Ning et al. 2013), the modified short-wave infrared perpendicular water stress index (MSPSI; Feng et al. 2013), the modified perpendicular drought index (MPDI; Ghulam et al. 2007), the normalized difference water index (NDWI; Rogers and Kearney 2004), and the moisture stress index (MSI; Hunt and Rock 1989).

Indices specifically designed for vegetation water content monitoring have been developed using NIR and SWIR bands, including the normalized difference infrared index (NDII; Hardisky, Michael Smart, and Klemas 1983), the global vegetation moisture index (GVMI; Ceccato et al. 2002; Ceccato, Flasse, and Grégoire 2002), and the NDWI (Gao 1996). Although this last index has been given the same name as the NDWI developed by Rogers and Kearney (2004), it is based on a different formula. Gao's NDWI is calculated as the normalized difference between NIR and SWIR bands, whereas Rogers and Kearney (2004) use red and SWIR bands to compute the NDWI (Lei, Zhang, and Bruce 2009). In our study, we used the NDWI definition given by Rogers and Kearney (2004).

In the literature, many indices based on NIR spectral reflectance have been developed to monitor soil moisture, such as the perpendicular drought index (PDI; Ghulam et al. 2007), the distance drought index (DDI; Yang et al. 2008), and the surface water content index (SWCI; Zhang et al. 2008; Du et al. 2013). These indices have proved to be efficient over bare soil surfaces (Qin et al. 2008; Zhang et al. 2008; Ghulam et al. 2008).

An operational index for simultaneously measuring the surface water content of bare soil, mixed bare, and covered soil has become crucial for irrigation management,

especially in arid and semi-arid regions. This is required, especially for large irrigated areas and throughout the cropping season, when the vegetation cover is continuously changing. An operational tool adapted to this context and that combines simplicity and robustness still deserves to be explored.

The main objective of this study was to explore the potential of NDWI and MSI for comparing, quantifying, and mapping the surface water content of wheat plots, from bare soil to completely covered soil. This index could lead to the development of an operational tool for monitoring surface water content and managing irrigation, at least for the study area.

2. Materials and methods

2.1. Study area

The study area is located in central Morocco (32°23′ N; 6°31′ W; 445 m above sea level), within the irrigation perimeter of the Tadla region. The area is characterized by a semi-arid climate; the annual average temperature is about 19°C, with large inter-seasonal variation. The average cropping season precipitation is about 300 mm (average over the 1970–2010 period), with significant inter-annual variation ranging from 130 to 600 mm. The area covers 100,000 ha and is characterized by a flat topography. The groundwater depth varies from 31 to 117 m (Bouchaou et al. 2009; Najine et al. 2006). Wheat is one of the main cultivated crops, covering 36% of the total cultivated land. As in the rest of Morocco, traditional flood irrigation is the dominant practice used in cereal plots. Generally, the wheat-growing cycle in the region starts in November and ends in June of the following calendar year, overlapping the rainy season. Wheat is irrigated two to five times, depending on water availability in autumn and winter and on amount of stored water in dams during the rainy season.

The area is divided into several hundred irrigation plots. For this study, 30 wheat plots were selected, with size varying from 1.7 to 24.5 ha (total area 117 ha). The diversity of crop management and irrigation schedules in these plots was representative of the general agricultural practices in the area.

Figure 1 shows the location of study area and illustrates the location of the selected plots. The plots were labelled from P1 to P26 and divided into 348 sub-plots of about 0.5 ha each. Plots P8, P9, P11, and P16 were monitored for two successive cropping seasons (2012–2013 and 2013–2014). The irrigation was managed by farmers. The irrigation duration ranged from 1 to 2 days ha^{-1}.

2.2. Soil data

In the study area, soil physics analyses were performed from 30 soil samples (Table 1) (Benabdelouahab 2009). These samples were collected from several sites providing coverage of the entire study area. Water content at permanent wilting point (PWP) and field capacity (FC) were measured using a pressure plate extractor. Soil reached PWP and FC when the water potential was at −1.5 and −0.033 MPa, respectively (Kirkham 2005).

On the basis of these analyses (Table 1), the soils are mainly homogeneous with fine texture (silty clay) which is characterized by a high water-holding capacity. The proportions of clay, silt, and sand, which together determine the soil textural class, present a high homogeneity, with a standard deviation of 3.40%, 2.69%, and 1.27%, respectively. The bulk density value is 1.21 (g cm^{-3}), with a standard deviation of 0.14. The strong

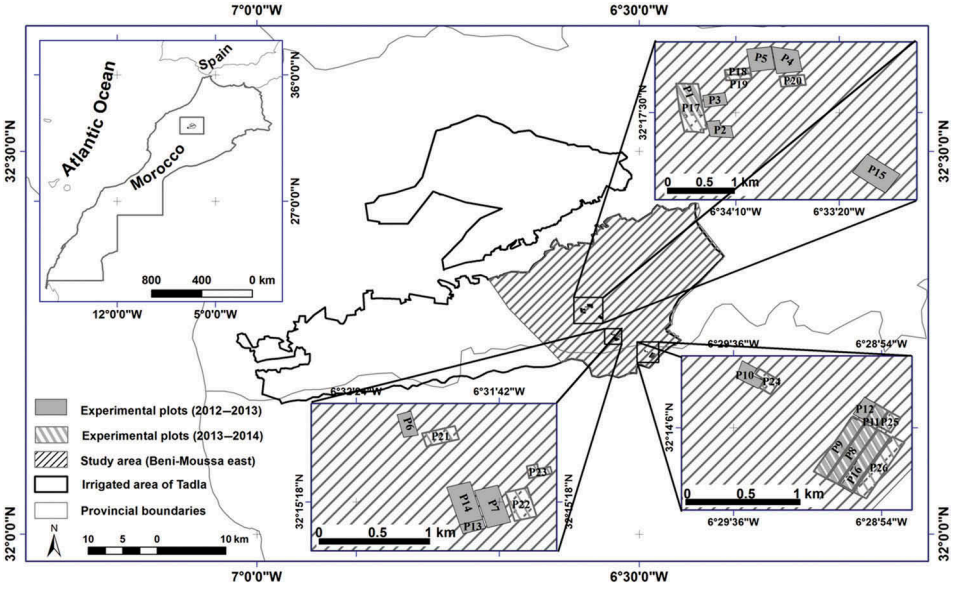

Figure 1. Location of the irrigated area (upper left inset shows a map of Morocco; the study area is indicated by diagonal lines and the experimental plots are in grey).

Table 1. Soil physics properties in Tadla, Morocco.

	Depth 0–30 cm		Depth 30–60 cm		Depth 60–100 cm	
Soil properties	Value	Standard deviation	Value	Standard deviation	Value	Standard deviation
Texture	Silty clay		Silty clay		Silty clay	
Sand (%)	25.35	2.69	24.53	1.90	23.96	0.29
Silt (%)	41.01	1.27	35.49	1.65	39.73	1.28
Clay (%)	33.64	3.40	39.99	1.26	36.31	1.51
Bulk density (g cm^{-3})	1.21	0.14	1.46	0.07	1.48	0.14
Field capacity (mm)	78.71	11.56	95.18	8.23	95.97	12.14
Saturation (mm)	106.02	4.23	118.13	4.84	124.8	5.55
Permanent wilting point (mm)	50.04	3.84	62.31	9.13	64.27	13.12
Hydraulic conductivity (cm h^{-1})	5.14	1.9	3.48	1.73	3.46	1.86

homogeneity of soil parameters in the study area justifies the use of the gravimetric soil moisture.

2.3. *Field data*

The experiments were conducted during the 2012–2013 and 2013–2014 wheat cropping seasons to assess changes in soil moisture and vegetation. Dates and levels of irrigation water supply and physiological crop data were collected.

Soil moisture was measured weekly for all 30 plots during the two cropping seasons, starting from sowing until grain filling, at 0–10 cm depth, with three random replications per plot. Soil moisture was measured using gravimetric methodology (dried in an oven at 105°C for 24 h). Vegetation water content was also measured weekly, starting from tillering until wheat grain filling (January–May 2013). In each plot, the vegetation water content was measured in four randomly selected quadrats (i.e. an area of 0.5 × 0.5 m). From each quadrat, sub-samples were used to measure the weight of the fresh and dry above-ground biomass in order to quantify vegetation water content (dried in an oven at 65°C for 48 h). Soil and vegetation water content were quantified on a gravimetric basis (i.e. g water/g soil or biomass), expressed as a percentage (%). These measurements were used to establish a relationship between vegetation water content and covered soil moisture.

The collected field data (soil moisture and vegetation water content) were vectorized as points and the experimental plots as polygons, in a geographical information system. Polygons were drawn so as to remove pixels falling along plot boundaries. The experimental plots were subdivided into sub-plot units of identical size (0.5 ha) and an identifier code was assigned to each of these units. Polygons of these sub-plot units served as a way of extracting pixel images that were close and directly linked to ground measurements.

Field data were collected in a regular and timely manner to ensure that ground measurements were acquired synchronously with satellite passes so as to obtain a good comparison between field measurements and remote-sensing data. Field measurements collected within a maximum of 3 days before or after a satellite pass were used for the analysis. We also ensured that during this period (between the field observation and the image acquisition date) there was no precipitation event or irrigation water supply.

2.4. *Satellite images and their processing*

Ten SPOT-5 HRV satellite images were acquired between December (at wheat emergence) and April (at grain filling) for the 2012–2013 and 2013–2014 cropping seasons (Table 2). They covered temporal changes in surface water content during the main wheat growth stages, except for the final senescent stage. The processing level of the acquired images was 1B, which included radiometric and geometric corrections. Atmospheric corrections were performed from radiance images, using the Fast Line-of-sight Atmospheric Analysis of Spectral Hypercubes (FLAASH) model available in the ENVI software. This model is considered to be more accurate for SPOT-5 images than other models (Guo and Zeng 2012).

Table 2. List of acquired SPOT-5 HRV images and their characteristics.

Acquisition date	Cropping season	Sensor	Wavelength (nm)	Spatial resolution (m)
12 December 2012	2012/2013	SPOT-5	Green: 500–590	Green: 10
2 February 2013		HRV	Red: 610–680	Red: 10
21 March 2013			NIR: 780–890	NIR: 10
26 March 2013			SWIR:1580–1750	SWIR: 20
11 April 2013				
2 December 2013	2013/2014			
6 January 2014				
1 February 2014				
26 March 2014				
15 April 2014				

Table 3. Spectral indices derived from the SPOT-5 sensor (red, NIR, and SWIR refer to the spectral reflectance bands of the SPOT-5 image).

Index	Abbreviation	Equation	Sensitivity	References
Normalized difference water index	NDWI	(Red – SWIR)/(Red + SWIR)	Vegetation water content and soil moisture content	Rogers and Kearney (2004), Lei, Zhang, and Bruce (2009), Lasaponara and Masini (2012)
Moisture stress index	MSI	(SWIR/NIR)	Vegetation water content	Ceccato et al. (2001), Ceccato et al. (2002), Hunt and Rock (1989)

The NDVI threshold method (Momeni and Saradjian 2007; Ning et al. 2013) was used to classify the land surface into three land-cover categories (Tables 4 and 5): bare soil (beginning of cropping season) with NDVI < 0.2; partly vegetated soil (mixed cover) with $0.2 \leq \text{NDVI} \leq 0.5$; and full vegetation cover with NDVI > 0.5.

The 12 December 2012 and 2 December 2013 images were acquired at the beginning of the growing season, when the soil was bare, whereas the 21 March 2013, 26 March 2013, 11 April 2013, 26 March 2014, and 15 April 2014 images were acquired when the soil was completely covered. The 2 February 2013, 6 January 2014, and 1 February 2014 images were acquired in the middle of the cropping season when the surface was partly covered by vegetation.

The visible spectrum (400–740 nm) is sensitive to vegetation water stress (Jensen 2005), with a more significant reflectance change in the red band (580–680 nm). The NIR band serves as a moisture-reference band, whereas the SWIR band is used as the moisture-measuring band. Reflectance in the NIR spectrum (740–1300 nm) is most sensitive to leaf internal structure changes (Jacquemoud and Baret 1990) and is insensitive to moisture variation (Elvidge and Lyon 1985), except in conditions leading to leaf dehydration which therefore affects leaf structure (Girard and Girard 2010; Jensen 2007). Recent studies confirmed the high sensitivity of the SWIR band to moisture variation in vegetation and soil (Ceccato et al. 2001; Cheng et al. 2013; Cheng, Rivard, and Sánchez-Azofeifa 2011; Yilmaz et al. 2008; Yilmaz, Hunt, and Jackson 2008; Hunt et al. 2011; Liu et al. 2012; Hunt and Rock 1989).

The first step in image post-processing involved computing two spectral indices, the NDWI (Rogers and Kearney 2004; Lasaponara and Masini 2012) and the MSI (Ceccato et al. 2001; Ceccato et al. 2002; Hunt and Rock 1989) (Table 3), using the spectral reflectance in the red, NIR, and SWIR bands for each SPOT-5 HRV image.

The second step involved delineating the region of interest (ROI) used as a mask of wheat sub-plots. The average values of the NDWI and MSI spectral indices were then computed for each corresponding sub-plot (7 × 7 pixels) where field measurements were conducted (Figure 2).

2.5. *Model calibration and evaluation*

The average MSI and NDWI values of the sub-plots and the corresponding ground measurements were compared using linear regression analysis. The regression coefficients a and b, reported in Tables 4 and 6, denote the slope and intercept of the regression line, respectively.

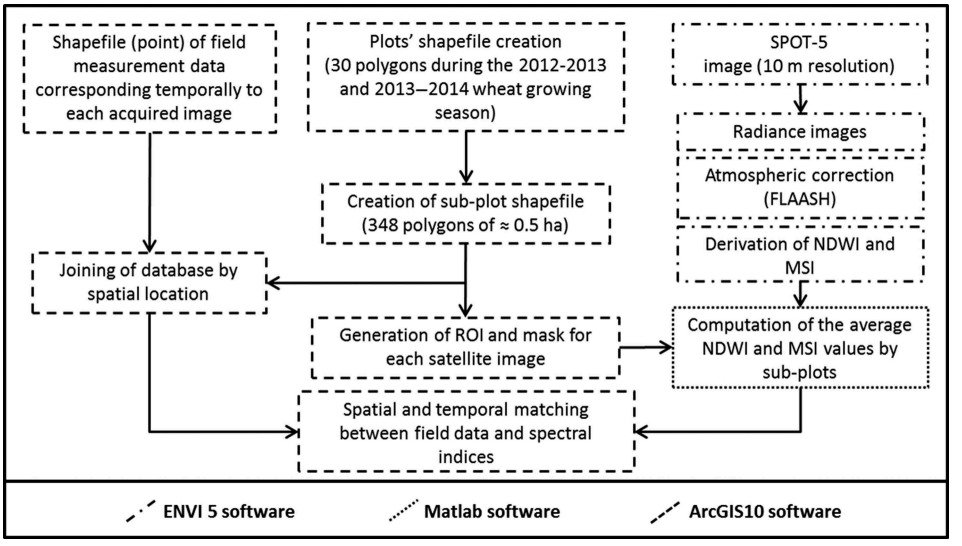

Figure 2. Schematic diagram illustrating field data and satellite image processing.

The statistics used for evaluating the regression models were: the coefficient of determination (R^2); the root mean square error (RMSE), which is one of the most widely used error assessment indices; and the normalized RMSE (nRMSE), expressed as a percentage of the RMSE divided by the mean of observed values (Richter et al. 2012):

$$\mathrm{RMSE} = \left[\sum_{i=1}^{n}(S_i - O_i)^2/n\right]^{0.5}, \tag{1}$$

$$\mathrm{nRMSE} = \left[\sum_{i=1}^{n}(S_i - O_i)^2/n\right]^{0.5} \times 100/M, \tag{2}$$

where S_i and O_i refer to simulated and observed values of the studied variable, respectively; i is an identifier varying from 1 to n; n is the number of observations; and M is the mean of the observed variable.

The value of nRMSE indicates the accuracy of the model and the dispersion around the mean of the observed values.

The accuracy of the regression models was evaluated using the k-fold cross-validation (k-fold CV) approach (Cassel 2007). Cross-validation is a resampling method that offers a different approach to model evaluation. It uses k replicate samples of observation data, builds models with $(k - 1)/k$ of data, and tests with the remaining $1/k$. The random k-fold CV takes k independent samples of size $N \times (k - 1)/k$ (Cassel 2007). In our study, it involved 33.3% of the observations as the validation data, with the remaining 66.6% of the observations being the training data, with 10 repetitions ($N = 10$).

2.6. Mapping soil moisture

Soil moisture was mapped using relationships of the validated linear regression models between satellite indices and ground measurements. The maps display surface soil moisture at plot level for each acquired satellite image.

3. Results and discussion

3.1. Soil moisture assessment at the beginning of wheat cropping season

The relationship between observed soil moisture and the MSI and NDWI values was assessed in 47 sub-plots at the beginning of the wheat cropping season (NDVI < 0.2), using images acquired on 12 December 2012 and 2 December 2013.

The reduced number of data used for this analysis is explained by the infrequent synchronization between field measurements and dates of satellite pass, particularly since only those measurements collected with a lag time of maximum 3 days from the date of satellite pass were considered.

As shown in Table 4, the R^2 and RMSE values were 0.84 ($p < 0.01$) and 1.03% for the NDWI and 0.79 ($p < 0.01$) and 1.18% for the MSI, respectively.

We compared the soil moisture values predicted using the *k*-fold CV method and those measured *in situ* (Table 5). The statistical indicators obtained from this comparison were $R^2 = 0.75$ ($p < 0.01$) and RMSE = 1.09% for NDWI and $R^2 = 0.73$ ($p < 0.01$) and RMSE = 1.24% for MSI. This comparison showed that errors were acceptable for both the MSI and NDWI, confirming the ability of these indices to accurately explain soil moisture variability for bare soil. Ghulam et al. (2007) reported similar results using the PDI and MPDI, with an R^2 of 0.56 and 0.55, respectively, over bare surfaces.

3.2. Vegetation water content and soil moisture assessment at full vegetation cover

The relationship between observed vegetation water content and MSI and NDWI was assessed in 62 sub-plots, when the soil was completely covered by vegetation (NDVI > 0.5). The statistical indicators obtained are presented in Table 6. The two spectral indices were strongly related to vegetation water content. The statistical indicators

Table 4. Linear regression analysis of the relationship between observed soil moisture and selected spectral indices.

		Number of samples	R^2	*a* (%)	*b* (%)	RMSE (%)	nRMSE (%)
NDWI	Bare soil (NDVI < 0.2)	47	0.84	−22.74	1.18	1.03	10.69
	Mixed cover (0.2 < NDVI < 0.5)	65	0.75	−13.85	8.3	1.38	7.22
	Completely covered soil (NDVI > 0.5)	100	0.83	−20.1	4.57	1.05	6.17
	All types of cover	212	0.86	−20.51	3.42	1.62	10.1
MSI	Bare soil (NDVI < 0.2)	47	0.79	2.04	1.26	1.18	12.23
	Mixed cover (0.2 < NDVI < 0.5)	65	0.38	2.4	21.75	2.04	10.80
	Completely covered soil (NDVI > 0.5)	100	0.68	−20.4	31.9	1.44	8.48
	All types of cover	212	0.49	−0.32	6.97	10.19	64.11

Table 5. The *k*-fold CV of the linear regression analysis of the relationship between observed soil moisture and selected spectral indices.

		Number of samples	R^2	RMSE (%)	nRMSE (%)
NDWI	Bare soil (NDVI < 0.2)	150	0.75	1.09	10.82
	Mixed cover (0.2 < NDVI < 0.5)	210	0.68	1.41	7.24
	Completely covered soil (NDVI > 0.5)	330	0.78	1.08	6.34
	All types of cover	700	0.85	1.61	10.01
MSI	Bare soil (NDVI < 0.2)	150	0.73	1.24	12.3
	Mixed cover (0.2 < NDVI < 0.5)	210	0.1	–	–
	Completely covered soil (NDVI > 0.5)	330	0.54	1.51	8.88
	All types of cover	700	0.05	–	–

Table 6. Linear regression analysis of the relationship between observed vegetation water content and selected spectral indices.

		Number of samples	R^2	*a* (%)	*b* (%)	RMSE (%)	nRMSE (%)
NDWI	Vegetation	62	0.77	−47.75	43.90	2.49	3.48
MSI			0.55	−34.98	97.57	3.47	4.85

Table 7. The *k*-fold CV of the linear regression analysis of the relationship between observed vegetation water content and the spectral indices.

		Number of samples	R^2	RMSE (%)	nRMSE (%)
NDWI	Vegetation	200	0.72	2.62	3.64
MSI			0.47	3.69	5.13

R^2 and RMSE were 0.77 ($p < 0.01$) and 2.49% for NDWI and 0.55 ($p < 0.01$) and 3.47% for MSI, respectively.

In order to validate these results, we compared observed vegetation water content values with those predicted using the *k*-fold CV method. As shown in Table 7, the errors were low for both NDWI and MSI. The evaluation model indicators obtained for predicted vegetation water content from NDWI were: RMSE of 2.62% and R^2 of 0.72 ($p < 0.01$). For MSI, the RMSE and R^2 values were 3.69% and 0.47 ($p < 0.01$), respectively. These results confirmed the ability of NDWI to estimate the vegetation water content for wheat, whereas the MSI values were less in agreement with the observed values. Similar results were reported for MSI by QiuXiang et al. (2012) and Hunt and Rock (1989).

Ning et al. (2013) reported the ability of the VSDI to simulate both soil moisture and vegetation water content, obtaining an R^2 of 0.51 and 0.42, respectively.

In areas with limited water availability, the critical period for wheat is during rapid growth, from the end of tillering to full stem elongation. In our study area, this corresponds to the period that usually begins in mid-March. Figure 3 compares measured soil moisture and wheat vegetation water content during the critical tillering to grain filling period. The figure shows a strong relationship between these two variables, with an R^2 of 0.82 ($p < 0.01$). During the development stages of healthy wheat, from tillering to grain

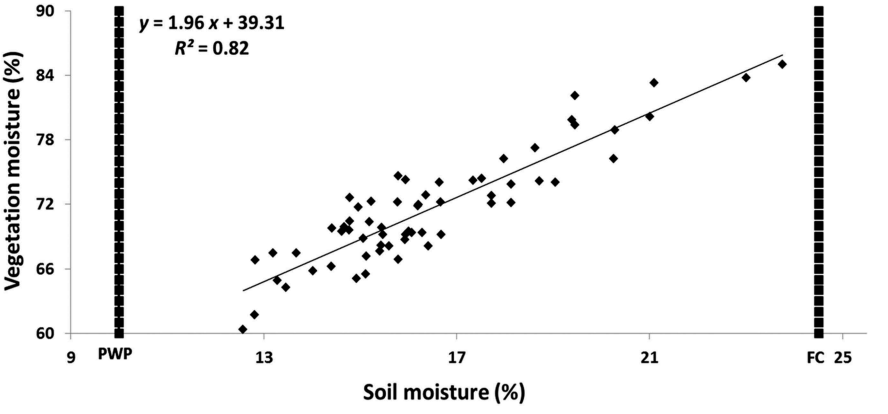

Figure 3. Relationship between vegetation and soil moisture measurements (FC, field capacity; PWP, permanent wilting point). Data were acquired on 21 March 2013, 26 March 2013, 11 April 2013, 26 March 2014, and 15 April 2014.

filling, and under the soil moisture conditions of the study area, the relationship was linear between FC (soil moisture of 24.3% at field capacity) and PWP (soil moisture of 9.8% at permanent wilting point), which accorded with the findings reported by Girard and Girard (2010). This shows that surface soil moisture can be estimated using vegetation water content and vice versa.

NDWI and MSI performed well in assessing top 10 cm soil moisture, when the soil was completely covered by vegetation. As shown in Table 4, R^2 and RMSE values were 0.83 ($p < 0.01$) and 1.05% for the NDWI and 0.68 ($p < 0.01$) and 1.44% for the MSI, respectively.

These results show the capacity of both NDWI and MSI to simultaneously estimate both vegetation water content and soil moisture, even when the soil is completely covered by the canopy, as confirmed by the *k*-fold validation results in Table 5.

Table 4 shows that change in land-cover type induced an MSI with opposing trends. As MSI uses the NIR band that behaves differently according to the type of cover (Ning et al. 2013), this index is not suitable for comparing different land-cover types simultaneously.

3.3. *Soil moisture assessment during the main growth stages of wheat*

Following the strong ability of NDWI and MSI to estimate soil moisture separately for bare soil and full vegetation cover, we tested the capacity of these spectral indices to estimate this parameter throughout the wheat cropping season, apart from the senescent stage which was not studied, since no irrigation is applied during this stage of wheat development.

Figures 4 and 6 show the comparison between observed soil moisture values and those derived using the spectral indices for the 10 acquisition dates. The statistical indicators R^2 and RMSE were 0.86 ($p < 0.01$) and 1.62% for NDWI, respectively (Table 4).

The point clouds for MSI, representing different kinds of cover, show opposite trends according to the main growth stages of wheat (Figure 6). This indicated that there was no unique linear relationship between MSI and surface soil moisture, for the entire wheat

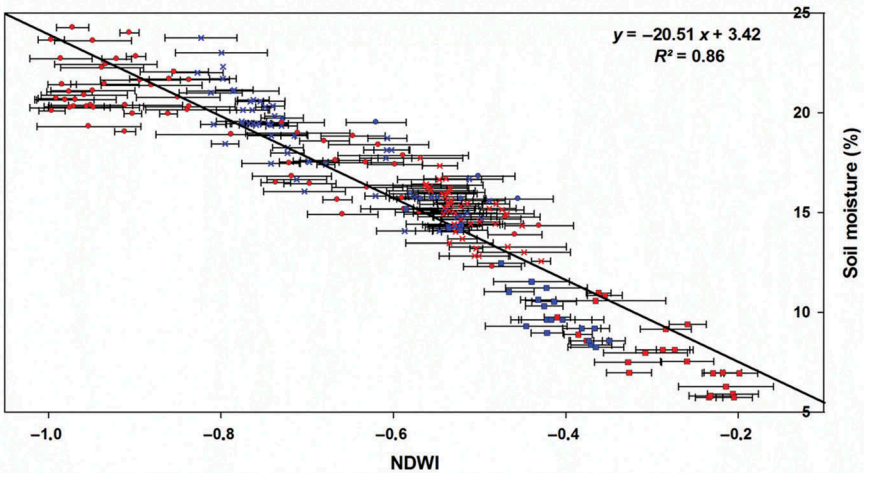

Figure 4. Relationship between soil moisture and NDWI values derived from all the acquired images (cropping season 2012–2013 in blue and cropping season 2013–2014 in red: squares, bare soil; cross, covered soil; circles, mixed cover). Error bars (based on standard deviation) show the range of NDWI values in each sub-plot.

crop cycle (apart from the senescent stage). The standard deviation of this index varies between 0.009 and 0.1 (Figure 6). The ratio between MSI values and the standard deviation expressed as a percentage varies between 0.23% and 11.88%.

In contrast, there was good agreement between NDWI and soil moisture, whatever the wheat growth stage, with standard deviation values ranging between 0.007 and 0.087 (Figure 4). The ratio between NDWI values and the standard deviation as a percentage ranges between 1.12% and 12.87%. The relationship was maintained from one year to the other (cf. Figure 4). The dispersion of the observed cloud points was mainly due to the spatial heterogeneity which characterized soil moisture at plot level (Bi et al. 2009; Xiaoning et al. 2009; Wang, Zhu, and Yan 2013), and the variable time lags ranging from 0 to 3 days between field measurement and satellite pass.

As shown in Table 4, the slope values (a) of the different types of cover for NDWI were relatively similar. For mixed cover, the slope was slightly steeper, indicating the stability of NDWI at different stages of crop cover (from emergence to grain filling) and its ability to quantify soil moisture throughout crop growth.

This finding was confirmed when comparing estimated and observed soil moisture using the k-fold CV approach (Figure 5). The statistics obtained for NDWI were RMSE = 1.61% and $R^2 = 0.85$ ($p < 0.01$).

With regard to MSI, the statistical analysis showed that this index is not suitable for estimating soil moisture throughout the crop-growing period, although it can accurately estimate bare soil moisture and vegetation water content separately (Figure 6). The NIR reflectance of covered soil is significantly higher than that of bare soil (Ning et al. 2013). As MSI uses NIR as the reference band, the values of this index are much higher for bare soil than for covered soil, which means that MSI cannot be used to compare dissimilar land-cover types.

Feng et al. (2013) simulated soil moisture using the MSPSI model and obtained an R^2 of 0.66. They also obtained R^2 values of 0.54, 0.48, and 0.60 for the PDI, MPDI, and SPSI models, respectively, for both bare and covered surfaces.

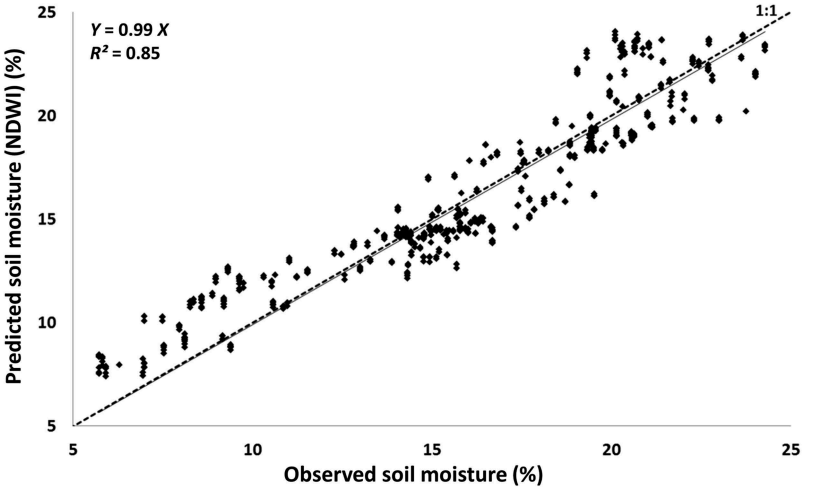

Figure 5. Comparison between observed and predicted soil moisture using the *k*-fold CV of all acquired images.

Ning et al. (2013) proposed using the VSDI for monitoring soil and vegetation moisture simultaneously over different land-cover types. This index is based on exploiting the SWIR and red bands. In a comparison between VSDI and the fractional water index over different land-cover types, they obtained an R^2 of 0.54.

3.4. *Mapping soil moisture*

Figures 7 and 8 show the soil moisture maps derived from the 10 SPOT-5 dates based on NDWI for the first (2012–2013) and second (2013–2014) cropping seasons, respectively. These maps were generated using a regression model (soil moisture = −20.51 × (NDWI) + 3.42) obtained by comparing the 10 available images and field measurements (see Figure 4). Soil moisture ranged from 6% (red) to 24% (blue). Figures 7(*f*) and 8(*f*) show the location of the plots.

The maps display change and variability in soil moisture between and within the plots, showing in particular differences between dry and wet plots. Such results could be very useful for monitoring water stress on a large scale for wheat and for detecting irrigation supplies.

In Figure 7(*a*), plots P1, P2, P3, P4, and P5 have a higher moisture content than other plots. This variation is caused by the first irrigation being applied before 12 December 2012, the date when the satellite image was acquired.

Some plots (P6, P7, P8, and P9) in Figure 7(*b*) show internal heterogeneity of the surface water content. The drying process is apparent in these plots, indicating the onset of water stress in the crop. This figure also shows heterogeneity among different plots, mainly due to irrigation supplies not being provided at the same time.

Figure 7(*b*) shows high soil moisture values, exceeding 16%, for plots P1, P2, P3, P4, and P15 in the red square and P10 in the blue square. These plots were irrigated during the last 10 days of January 2013. This was the second irrigation applied by farmers in the study area. Plot P4 did not appear to be completely irrigated at this time, indicating that

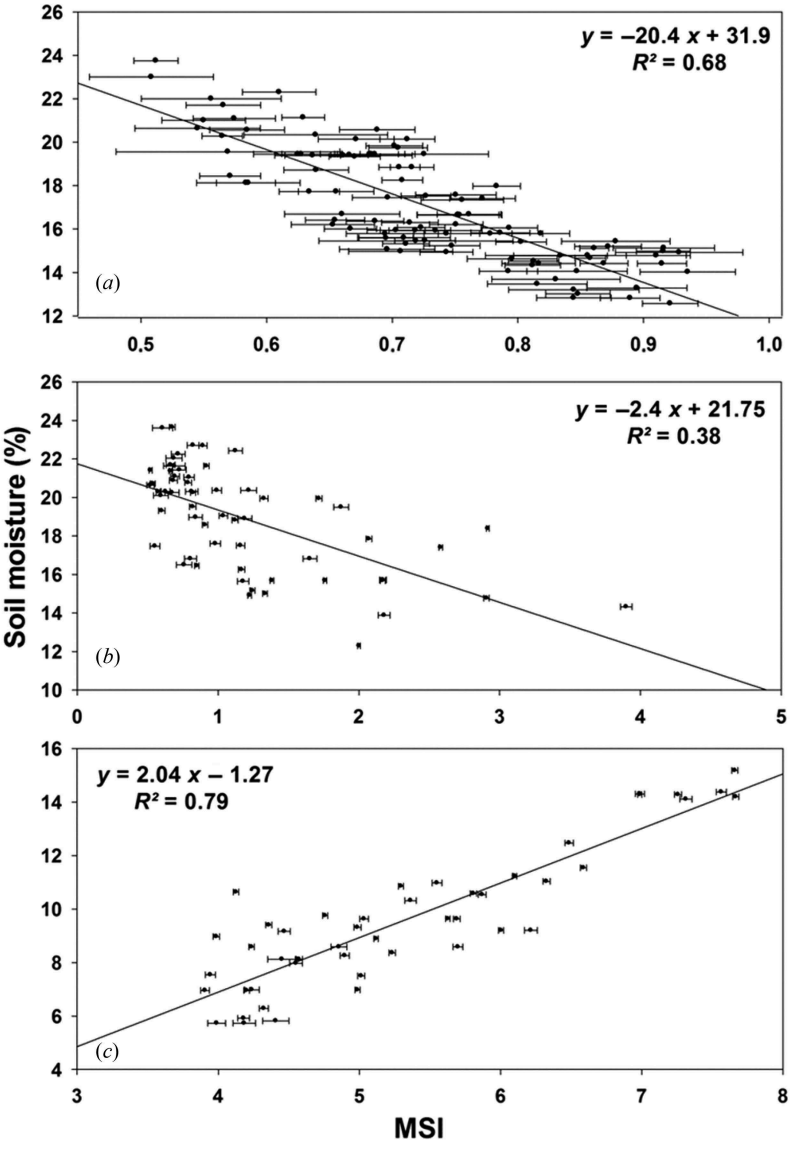

Figure 6. Relationship between soil moisture and the MSI values derived from all the acquired images: (*a*) covered soil; (*b*) mixed cover; and (*c*) bare soil. Error bars (based on standard deviation) show the range of MSI values in each sub-plot.

irrigation was in progress on the image acquisition date. The other plots were irrigated in January or after 2 February 2013, the date of the satellite pass.

Figures 7(*c*) and 7(d) show significant homogeneity and a dominance of blue, indicating that soil moisture was high (20–24%). This is explained by rainfall that occurred between 14 and 18 March 2013 (31.3 mm) and on 24 March 2013 (14 mm). These dates correspond to the dates when images were acquired (i.e. 21 and 26 March 2013). Figure 7(*e*) shows that after two weeks of rainfall, there was a homogeneous drying

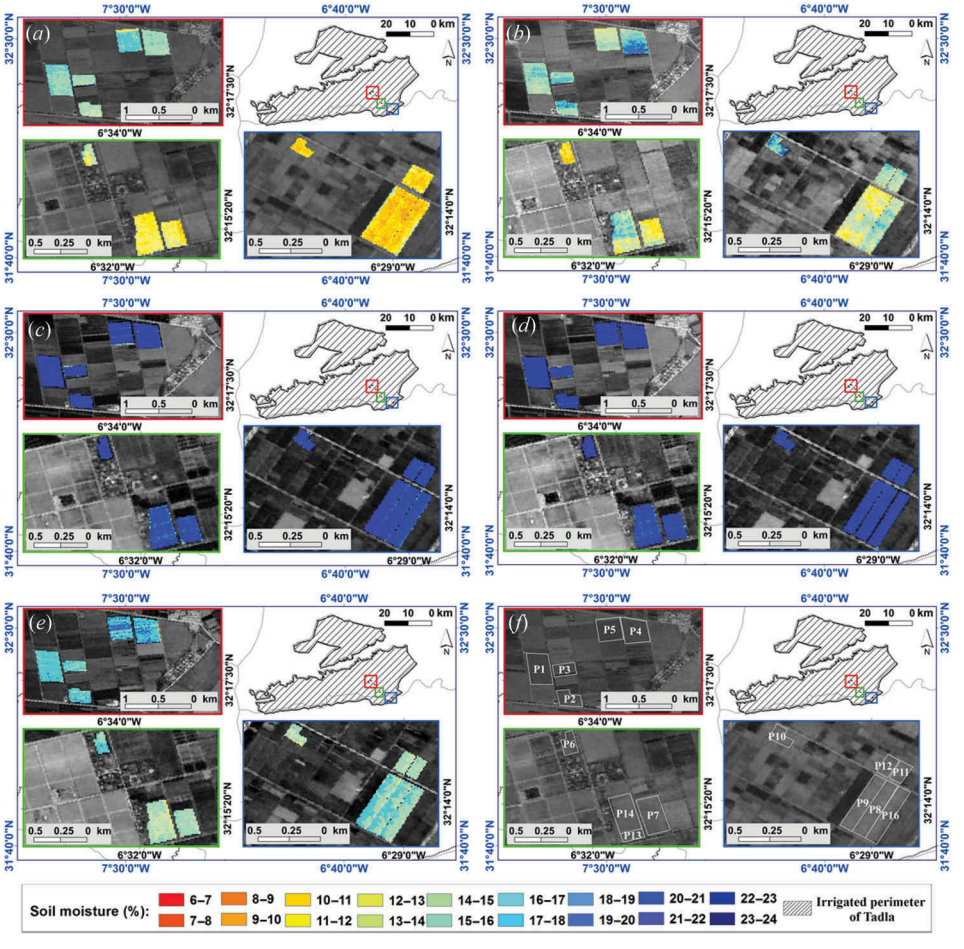

Figure 7. Soil moisture maps derived from the NDWI data: (*a*) 12 December 2012; (*b*) 2 February 2013; (*c*) 21 March 2013; (*d*) 26 March 2013; (*e*) 11 April 2013; and (*f*) codes for the experimental plots.

of the plots, with soil moisture ranging from 14% to 16%. The drying process was somewhat attenuated for plots P4 and P5, which were irrigated by the end of March.

In Figure 8(*a*), some pixels in P24 displayed quite a high surface water content level (16−18%), explained by the first irrigation. In wheat fields, irrigation water is supplied straight after sowing. Thus, the detection of the first irrigation can generally indicate the sowing date.

In Figure 8(*b*), it is interesting to note that plot P17 appears to be partly irrigated, indicating that irrigation was in progress. Plots P8, P9, P11, P16, P18, P19, P20, P24, and P25 were irrigated a few days before acquisition of the satellite image on 6 January 2014.

Figure 8(*c*), derived from the satellite image acquired on 1 February 2014, shows high and homogeneous surface water content (20–24%). This is explained by significant rainfall that occurred between 30 and 31 January 2014 (36.5 mm).

Both Figures 8(*d*) and 8(e), derived from images acquired on 26 March 2014 and 15 April 2014, show relatively low humidity, ranging from 12% to 15%. This can be

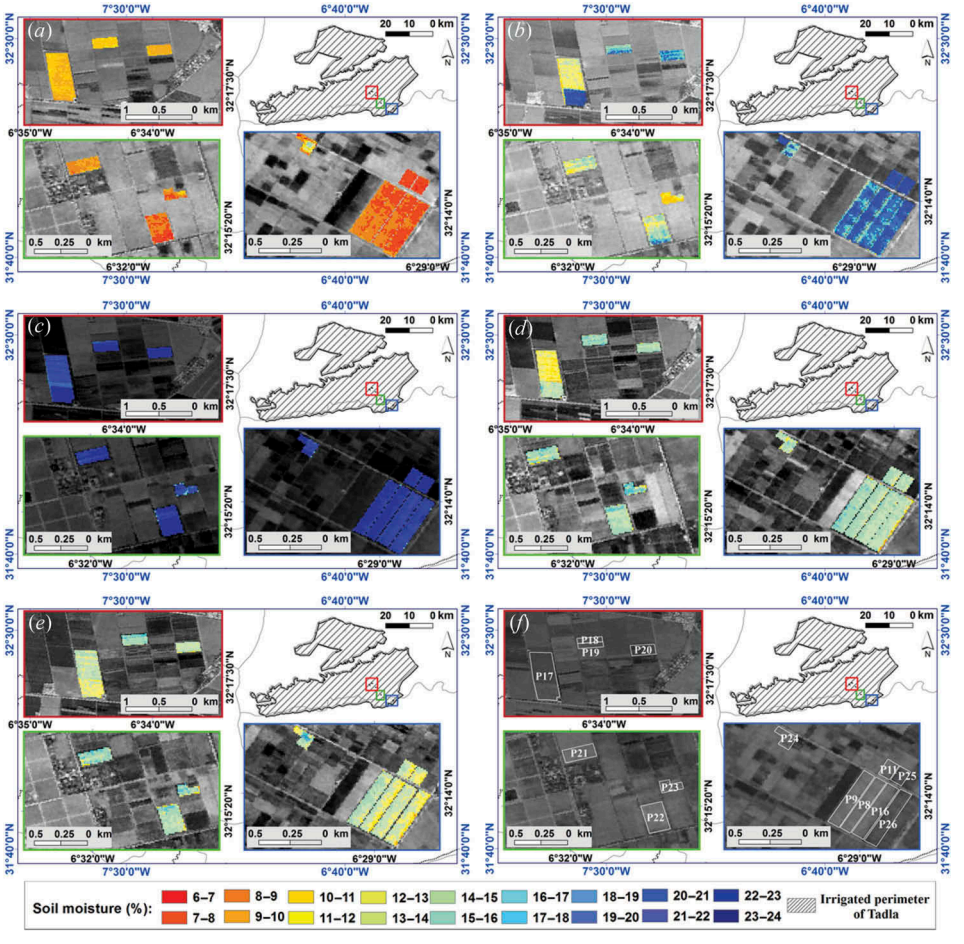

Figure 8. Soil moisture maps derived from the NDWI data: (*a*) 2 December 2013; (*b*) 6 January 2014; (*c*) 1 February 2014; (*d*) 26 March 2014; (*e*) 15 April 2014; and (*f*) codes for the experimental plots.

explained by irrigation that was scheduled at the beginning of March and after mid-April, in addition to lack of rainfall for a period of 12 days before the date of image acquisition. These figures portray the process of drying and the start of water stress of the wheat crop.

The developed method can be used as an operational tool for managing irrigation and crops and monitoring the evolution of surface water content at the plot scale, as well as on a larger scale across the irrigated area.

The practical aspects of this method that could improve irrigation water management in an irrigated perimeter include the following:

- The method can be used for triggering irrigation supplies in water stress situations and otherwise prevent contributions in excess of irrigation water. Such information could be valuable for decision-makers in charge of irrigation and crop management in irrigated areas.

- It could also be useful for detecting illegal irrigation and pumping. This is relevant in irrigated areas where irrigation has not been scheduled and uncontrolled water pumping is prohibited.
- It could also be used for detecting the date of sowing, which is usually concomitant with the first irrigation.

4. Conclusions

This study sought to assess the ability of two spectral indices, NDWI and MSI, derived from SPOT-5 HRV satellite images, to estimate surface water content from bare soil to completely covered soil throughout the cropping season in irrigated semi-arid areas.

The comparison between NDWI, using the red and SWIR bands, and soil moisture measurements at a depth of 0–10 cm throughout the cropping season showed good agreement, with an R^2 of 0.86. MSI appeared to be less suitable for quantifying and comparing soil moisture content at different stages during the wheat cycle. This index could be used, however, to estimate bare soil moisture, covered soil moisture, and vegetation water content separately. The derived soil moisture maps showed interesting spatial patterns that could be related to the dates of irrigation and rainfall events in the irrigated perimeter of Tadla.

NDWI can be used to compare, quantify, and map surface water content, at different stages of crop cover (from sowing to grain filling) over several years. It shows potential for improving irrigation monitoring, detecting irrigation supplies, wheat stress management, and our understanding of surface water content changes at field and regional levels in the study area. The performance of the methodology should be checked in other contexts before judging its suitability for application in other areas.

Acknowledgements

This work was supported by the Belgian Technical Cooperation Agency and the National Institute for Agronomic Research of Morocco. The acquisition of SPOT-5 images was supported by the ISIS programme of the National Centre for Space Studies (CNES). The authors are indebted to the staff of the Regional Centre for Agronomic Research of Tadla for their collaboration, as well as to Mrs Marie Lang and Mr Abdul Aziz Diouf for their valuable help and Mr Hassan Noury who participated in field measurements.

Disclosure statement

No potential conflict of interest was reported by the authors.

References

Balaghi, R., M. C. Badjeck, D. Bakari, E. De Pauw, A. De Wit, P. Defourny, S. Donato, R. Gommes, M. Jlibene, A. C. Ravelo, M. V. K. Sivakumar, N. Telahigue, and B. Tychon. 2010. "Managing Climatic Risks for Enhanced Food Security: Key Information Capabilities." *Procedia Environmental Sciences* 1: 313–323. doi:10.1016/j.proenv.2010.09.020.

Balaghi, R., M. Jlibene, B. Tychon, and H. Eerens. 2013. *Agrometeorological Cereal Yield Forecasting in Morocco*. Rabat: INRA.

Benabdelouahab, T. 2009. "Spatialisation des paramètres hydrodynamiques des sols du périmètres irrigué du Tadla par les méthodes géostatistiques." In *INRA Research Activities Report*, edited by INRA, 87. Rabat: INRA.

Ben-Gal, A., D. Kool, N. Agam, G. E. van Halsema, U. Yermiyahu, A. Yafe, E. Presnov, R. Erel, A. Majdop, I. Zipori, E. Segal, S. Rüger, U. Zimmermann, Y. Cohen, V. Alchanatis, and A. Dag. 2010. "Whole-Tree Water Balance and Indicators for Short-Term Drought Stress in Non-Bearing 'Barnea' Olives." *Agricultural Water Management* 98 (1): 124–133. doi:10.1016/j.agwat.2010.08.008.

Bi, H., X. Li, X. Liu, M. Guo, and J. Li. 2009. "A Case Study of Spatial Heterogeneity of Soil Moisture in the Loess Plateau, Western China: A Geostatistical Approach." *International Journal of Sediment Research* 24 (1): 63–73. doi:10.1016/S1001-6279(09)60016-0.

Bouchaou, L., J. L. Michelot, M. Qurtobi, N. Zine, C. B. Gaye, P. K. Aggarwal, H. Marah, A. Zerouali, H. Taleb, and A. Vengosh. 2009. "Origin and Residence Time of Groundwater in the Tadla Basin (Morocco) Using Multiple Isotopic and Geochemical Tools." *Journal of Hydrology* 379 (3–4): 323–338. doi:10.1016/j.jhydrol.2009.10.019.

Cassel, D. L. 2007. "Re-Sampling and Simulation, the SAS Way." Paper presented at the Proceedings of the SAS Global Forum 2007 Conference, Cary, NC, May 17.

Ceccato, P., S. Flasse, and J. M. Grégoire. 2002. "Designing a Spectral Index to Estimate Vegetation Water Content from Remote Sensing Data: Part 2. Validation and Applications." *Remote Sensing of Environment* 82 (2–3): 198–207. doi:10.1016/S0034-4257(02)00036-6.

Ceccato, P., S. Flasse, S. Tarantola, S. Jacquemoud, and J. M. Grégoire. 2001. "Detecting Vegetation Leaf Water Content Using Reflectance in the Optical Domain." *Remote Sensing of Environment* 77 (1): 22–33. doi:10.1016/S0034-4257(01)00191-2.

Ceccato, P., N. Gobron, S. Flasse, B. Pinty, and S. Tarantola. 2002. "Designing a Spectral Index to Estimate Vegetation Water Content from Remote Sensing Data: Part 1: Theoretical Approach." *Remote Sensing of Environment* 82: (2–3): 188-97. doi:10.1016/S0034-4257(02)00037-8.

Cheng, T., D. Riaño, A. Koltunov, M. L. Whiting, S. L. Ustin, and J. C. Rodriguez. 2013. "Detection of Diurnal Variation in Orchard Canopy Water Content Using MODIS/ASTER Airborne Simulator (MASTER) Data." *Remote Sensing of Environment* 132: 1–12. doi:10.1016/j.rse.2012.12.024.

Cheng, T., B. Rivard, and A. Sánchez-Azofeifa. 2011. "Spectroscopic Determination of Leaf Water Content Using Continuous Wavelet Analysis." *Remote Sensing of Environment* 115 (2): 659–670. doi:10.1016/j.rse.2010.11.001.

Cheng, T., B. Rivard, A. G. Sánchez-Azofeifa, J. B. Féret, S. Jacquemoud, and S. L. Ustin. 2012. "Predicting Leaf Gravimetric Water Content from Foliar Reflectance across a Range of Plant Species Using Continuous Wavelet Analysis." *Journal of Plant Physiology* 169 (12): 1134–1142. doi:10.1016/j.jplph.2012.04.006.

Du, L., Q. Tian, T. Yu, Q. Meng, T. Jancso, P. Udvardy, and Y. Huang. 2013. "A Comprehensive Drought Monitoring Method Integrating MODIS and TRMM Data." *International Journal of Applied Earth Observation and Geoinformation* 23: 245–253. doi:10.1016/j.jag.2012.09.010.

Elvidge, C. D., and R. J. P. Lyon. 1985. "Influence of Rock-Soil Spectral Variation on the Assessment of Green Biomass." *Remote Sensing of Environment* 17 (3): 265–279. doi:10.1016/0034-4257(85)90099-9.

Er-Raki, S., A. Chehbouni, and B. Duchemin. 2010. "Combining Satellite Remote Sensing Data with the FAO-56 Dual Approach for Water Use Mapping in Irrigated Wheat Fields of a Semi-Arid Region." *Remote Sensing* 2 (1): 375–387. doi:10.3390/rs2010375.

Feng, H., C. Chen, H. Dong, J. Wang, and Q. Meng. 2013. "Modified Shortwave Infrared Perpendicular Water Stress Index: A Farmland Water Stress Monitoring Method." *Journal of Applied Meteorology and Climatology* 52 (9): 2024–2032. doi:10.1175/jamc-d-12-0164.1.

Gao, B. C. 1996. "NDWI - A Normalized Difference Water Index for Remote Sensing of Vegetation Liquid Water from Space." *Remote Sensing of Environment* 58 (3): 257–266. doi:10.1016/S0034-4257(96)00067-3.

Geerts, S., and D. Raes. 2009. "Deficit Irrigation as On-Farm Strategy to Maximize Crop Water Productivity in Dry Areas." *Agricultural Water Management* 96: 1275–1284. doi:10.1016/j.agwat.2009.04.009.

Ghulam, A., Q. Qin, T. Kuskya, and Z. Li. 2008. "A Re-Examination of Perpendicular Drought Indices." *International Journal of Remote Sensing* 29: 6037–6044. doi:doi:10.1080/01431160802235811.

Ghulam, A., Q. Qin, T. Teyip, and Z. L. Li. 2007. "Modified Perpendicular Drought Index (MPDI): A Real-Time Drought Monitoring Method." *ISPRS Journal of Photogrammetry and Remote Sensing* 62 (2): 150–164. doi:10.1016/j.isprsjprs.2007.03.002.

Girard, M.-C., and C.-M. Girard. 2010. *Traitement des données de télédétection: Environnement et ressources naturelles*. 2 ed., edited by Dunod. Paris: Dunod. *Environnement et sécurité*.

Guo, Y., and F. Zeng. 2012. "Atmospheric Correction Comparison of SPOT-5 Image Based on Model FLAASH and Model QUAC." *International Archives of the Photogrammetry and Remote Sensing Spatial Information Science* XXXIX-B7: 7–11. doi:10.5194/isprsarchives-XXXIX-B7-7-2012.

Hadria, R., B. Duchemin, L. Jarlan, G. Dedieu, F. Baup, S. Khabba, A. Olioso, and T. Le Toan. 2010. "Potentiality of Optical and Radar Satellite Data at High Spatio-Temporal Resolutions for the Monitoring of Irrigated Wheat Crops in Morocco." *International Journal of Applied Earth Observation and Geoinformation* 12 (1): S32–S37. doi:10.1016/j.jag.2009.09.003.

Hardisky, M. A., R. Michael Smart, and V. Klemas. 1983. "Growth Response and Spectral Characteristics of a Short Spartina Alterniflora Salt Marsh Irrigated with Freshwater and Sewage Effluent." *Remote Sensing of Environment* 13 (1): 57–67. doi:10.1016/0034-4257(83)90027-5.

Hunt, E. R. Jr, L. Li, M. T. Yilmaz, and T. J. Jackson. 2011. "Comparison of Vegetation Water Contents Derived from Shortwave-Infrared and Passive-Microwave Sensors over Central Iowa." *Remote Sensing of Environment* 115 (9): 2376–2383. doi:10.1016/j.rse.2011.04.037.

Hunt, E. R. Jr, and B. N. Rock. 1989. "Detection of Changes in Leaf Water Content Using Near- and Middle-Infrared Reflectances." *Remote Sensing of Environment* 30 (1): 43–54. doi:10.1016/0034-4257(89)90046-1.

Jacquemoud, S., and F. Baret. 1990. "PROSPECT: A Model of Leaf Optical Properties Spectra." *Remote Sensing of Environment* 34 (2): 75–91. doi:10.1016/0034-4257(90)90100-Z.

Jensen, J. R. 2005. *Introductory Digital Image Processing: A Remote Sensing Perspective*. 3rd ed. Upper Saddle River, NJ: Prentice-Hall.

Jensen, J. R. 2007. *Remote Sensing of the Environment: An Earth Resource Perspective*. 2nd ed. Upper Saddle River, NJ: Prentice Hall.

Kirkham, M. B. 2005. "8 - Field Capacity, Wilting Point, Available Water, and the Nonlimiting Water Range." In *Principles of Soil and Plant Water Relations*, edited by M. B. Kirkham, 101–115. Burlington, MA: Academic Press.

Kogan, F. N. 2000. "Contribution of Remote Sensing to Drought Early Warning." Paper presented at the Early Warning Systems for Drought Preparedness and Drought Management, Lisbon, September 5–7.

Lasaponara, R., and N. Masini, eds. 2012. *Satellite Remote Sensing: A New Tool for Archaeology*. Dordrecht: Springer.

Lei, J., L. Zhang, and W. Bruce. 2009. "Analysis of Dynamic Thresholds for the Normalized Difference Water Index." *Photogrammetric Engineering & Remote Sensing* 75: 1307–1317. doi:10.14358/PERS.75.11.1307.

Lionboui, H., A. Fadlaoui, F. Elame, and T. Benabdelouahab. 2014. "Water Pricing Impact on the Economic Valuation of Water Resources." *International Journal of Education and Research* 2 (6): 147–166.

Liu, S., D. A. Roberts, O. A. Chadwick, and C. J. Still. 2012. "Spectral Responses to Plant Available Soil Moisture in a Californian Grassland." *International Journal of Applied Earth Observation and Geoinformation* 19: 31–44. doi:10.1016/j.jag.2012.04.008.

Lobell, D. B., G. P. Asner, J. I. Ortiz-Monasterio, and T. L. Benning. 2003. "Remote Sensing of Regional Crop Production in the Yaqui Valley, Mexico: Estimates and Uncertainties." *Agriculture, Ecosystems and Environment* 94: 205–220. doi:10.1016/S0167-8809(02)00021-X.

Momeni, M., and M. R. Saradjian. 2007. "Evaluating Ndvi-Based Emissivities of MODIS Bands 31 and 32 Using Emissivities Derived by Day/Night LST Algorithm." *Remote Sensing of Environment* 106 (2): 190–198. doi:10.1016/j.rse.2006.08.005.

Moreno, A., F. Maselli, M. Chiesi, L. Genesio, F. Vaccari, G. Seufert, and M. A. Gilabert. 2014. "Monitoring Water Stress in Mediterranean Semi-Natural Vegetation with Satellite and Meteorological Data." *International Journal of Applied Earth Observation and Geoinformation* 26: 246–255. doi:10.1016/j.jag.2013.08.003.

Muller, E., and H. Décamps. 2001. "Modeling Soil Moisture-Reflectance." *Remote Sensing of Environment* 76: 173–180. doi:10.1016/S0034-4257(00)00198-X.

Najine, A., M. Jaffal, K. E. Khammari, T. Aïfa, D. Khattach, M. Himi, A. Casas, S. Badrane, and H. Aqil. 2006. "Contribution de la gravimétrie à l'étude de la structure du bassin de Tadla (Maroc) :

Implications hydrogéologiques." *Comptes Rendus Geoscience* 338 (10): 676–682. doi:10.1016/j.crte.2006.04.015.

Ning, Z., H. Yang, Q. Qiming, and L. Lu. 2013. "VSDI: A Visible and Shortwave Infrared Drought Index for Monitoring Soil and Vegetation Moisture Based on Optical Remote Sensing." *International Journal of Remote Sensing* 34: 4585–4609. doi:10.1080/01431161.2013.779046.

ORMVAT. 2009. "Rapport annuel de l'Office de la mise en valeur agricole de Tadla." *ORMVAT Activities Report 27.*

Ozdogan, M., Y. Yang, G. Allez, and C. Cervantes. 2010. "Remote Sensing of Irrigated Agriculture: Opportunities and Challenges." *Remote Sensing* 2 (9): 2274–2304. doi:10.3390/rs2092274.

Penuelas, J., J. Pinol, R. Ogaya, and I. Filella. 1997. "Estimation of Plant Water Concentration by the Reflectance Water Index WI (R900/R970)." *International Journal of Remote Sensing* 18 (13): 2869–2875. doi:10.1080/014311697217396.

Qin, Q., A. Ghulam, L. Zhu, L. Wang, J. Li, and P. Nan. 2008. "Evaluation of MODIS Derived Perpendicular Drought Index for Estimation of Surface Dryness Over Northwestern China." *International Journal of Remote Sensing* 29: 1983–1995. doi:doi:10.1080/01431160701355264.

QiuXiang, Y., B. AnMing, L. Yi, and Z. Jin. 2012. "Measuring Cotton Water Status Using Water-Related Vegetation Indices at Leaf and Canopy Levels." *Journal of Arid Land* 4 (3): 310−9. doi:10.3724/SP.J.1227.2012.00310.

Richter, K., C. Atzberger, T. B. Hank, and W. Mauser. 2012. "Derivation of Biophysical Variables from Earth Observation Data: Validation and Statistical Measures." *Journal of Applied Remote Sensing* 6 (1): 063557–23. doi:10.1117/1.jrs.6.063557.

Rogers, A. S., and M. S. Kearney. 2004. "Reducing Signature Variability in Unmixing Coastal Marsh Thematic Mapper Scenes Using Spectral Indices." *International Journal of Remote Sensing* 25 (12): 2317–2335. doi:10.1080/01431160310001618103.

Seckler, D., R. Barker, and U. Amarasinghe. 1999. "Water Scarcity in the Twenty-First Century." *International Journal of Water Resources Development* 15: 29–42. doi:10.1080/07900629948916.

Skidmore, E. L., J. D. Dickerson, and H. Shimmelpfennig. 1975. "Evaluating Surface-Soil Water Content by Measuring Reflectance." *Soil Science Society of American Proceedings* 39: 238–242. doi:10.2136/sssaj1975.03615995003900020009x.

Tian, Q., Q. Tong, R. Pu, X. Guo, and C. Zhao. 2001. "Spectroscopic Determination of Wheat Water Status Using 1650-1850 Nm Spectral Absorption Features." *International Journal of Remote Sensing* 22 (12): 2329–2338. doi:10.1080/01431160118199.

Trombetti, M., D. Riaño, M. A. Rubio, Y. B. Cheng, and S. L. Ustin. 2008. "Multi-Temporal Vegetation Canopy Water Content Retrieval and Interpretation Using Artificial Neural Networks for the Continental USA." *Remote Sensing of Environment* 112 (1): 203–215. doi:10.1016/j.rse.2007.04.013.

Wang, Y.-G., H. Zhu, and L. Yan. 2013. "Spatial Heterogeneity of Soil Moisture, Microbial Biomass Carbon and Soil Respiration at Stand Scale of an Arid Scrubland." *Environmental Earth Sciences* 70 (7): 3217–3224. doi:10.1007/s12665-013-2386-z.

Xiaoning, S., Z. Xia, L. Xiaotao, and L. Xinhui. 2009. "Spatial Heterogeneity Analysis of Soil Moisture Based on Geostatistics." Paper presented at 2009 1st International Conference on Information Science and Engineering (ICISE), Nanjing, December 26–28.

Yang, N., Q. Qin, C. Jin, and Y. Yao. 2008. "The Comparison and Application of the Methods for Monitoring Farmland Drought Based on NIR-Red Spectral Space." *International Geoscience and Remote Sensing Symposium (IGARSS 2008)* III871–III4. doi:10.1109/IGARSS.2008.4779488.

Yilmaz, M. T., E. R. Hunt Jr, L. D. Goins, S. L. Ustin, V. C. Vanderbilt, and T. J. Jackson. 2008. "Vegetation Water Content during SMEX04 from Ground Data and Landsat 5 Thematic Mapper Imagery." *Remote Sensing of Environment* 112 (2): 350–362. doi:10.1016/j.rse.2007.03.029.

Yilmaz, M. T., E. R. Hunt Jr, and T. J. Jackson. 2008. "Remote Sensing of Vegetation Water Content from Equivalent Water Thickness Using Satellite Imagery." *Remote Sensing of Environment*. 112 (5): 2514–2522. doi:10.1016/j.rse.2007.11.014.

Zhang, H., H. Chen, S. Shen, G. Zhou, and W. Yu. 2008. "Drought Remote Sensing Monitoring Based on the Surface Water Content Index (SWCI) Method." *Remote Sensing Technology and Application* 23: 624–628.